

# On the Suitability of Thermogravimetric Balances for the Study of Biomass Pyrolysis

Meredith R. Barr<sup>1</sup>, Maurizio Volpe<sup>2</sup>, Antonio Messineo<sup>2</sup> and Roberto Volpe<sup>1,\*</sup>

## Abstract

In fixed-bed pyrolysis reactors, the stacking of sample particles often leads to higher yields of solid pyrolysis products (chars) than are obtained from other types of reactors. This phenomenon is particularly emphasised in thermogravimetric (TG) balances, which unlike many fixed-bed reactors, do not sweep gas through the stationary bed of pyrolysing sample. Gas is swept through the sample bed to reduce the residence time of tar vapours in close proximity to chars, which affects the extent to which these vapours will condense onto the surface of chars and repolymerise, thus increasing char yield. Depth of the sample bed affects this residence time, and thus affects char yield. In this work, the sensitivity of typical analyses of biomass thermogravimetry to variations in bed depth have been assessed. Results of these analyses, including product distributions, proximate compositions, and kinetic predictions, carried out on microcrystalline cellulose and birch wood hydrochar samples produced at temperatures ranging from 160 to 280 °C, have been shown to be sensitive to variations in bed depth, and it has been demonstrated that this sensitivity is amplified at higher heating rates and temperatures. Thus, when a single sample mass is used for any of these typical TG analyses, as is common in published literature, the results are not fundamental properties of the material tested but rather a product of the exact experimental design employed. Future work is needed to identify reactor and experimental design guidelines to minimise this sensitivity in fixed-bed reactors.

**Keywords:** Thermogravimetric analysis (TGA), Pyrolysis, Biomass, Fixed-bed reactors, Kinetics, Proximate analysis

---

<sup>1</sup>Queen Mary University of London, Mile End Road, London E1 4NS, UK

<sup>2</sup>Università degli Studi di Enna "Kore", Cittadella Universitaria, 94100 Enna

\*Corresponding author. Email address: r.volpe@qmul.ac.uk

## 1. Introduction

Thermogravimetric analysis (TGA) is a popular and convenient technique for the study of biomass pyrolysis. Advanced thermogravimetric (TG) balances can run dozens of samples in sequence, while collecting and auto-analysing time-resolved yield and gas-composition data without operator intervention. Because of this, TGA is widely used for biomass characterisation and the study of biomass pyrolysis. In particular, TGA is often used to compare the properties of different biomass feedstocks for thermochemical conversion,<sup>1,2</sup> to track the evolution of the solid state throughout thermochemical conversion processes,<sup>3,4</sup> and to measure the apparent kinetics of thermochemical conversion reactions.<sup>5-9</sup> Despite the attractive features of TG balances, their configuration damages their accuracy and fidelity. This work demonstrates the effects of this configuration on the results of typical analyses of biomass thermogravimetry, including char yields, kinetic predictions, and proximate compositions.

### *1.1. Particle Stacking in Fixed-Bed Reactors*

TG balances are often used as fixed-bed pyrolysis reactors, which are defined by a stationary bed of sample, as opposed to a fluidised bed in which sample particles can move freely throughout the heated region. This fixed-bed configuration inherently leads to stacking of sample particles, which substantially affects the mechanism of pyrolysis.<sup>10</sup>

Primary pyrolysis processes produce liquid-phase tars, composed principally of monomers and oligomers of lignocellulosic components (cellulose, hemicellulose, and lignin). Volatilised tars in the gas phase may either crack to form lighter volatiles, or condense onto a surface. When tars condense back onto the surface of chars, they may repolymerise, resulting in increased char yield. This reactivity of tar in the presence of char has been demonstrated by numerous researchers.<sup>11-15</sup> In this way, the more time gas-phase pyrolysis products spend in close proximity to char particles (the sample bed), the greater char yield will be, and any experimental parameter that affects this residence time, will thus affect char yield.<sup>16-19</sup>

To minimise the effect of repolymerisation on char yield, inert gas is often flowed through the sample bed to sweep away gas-phase tars, but in fixed-bed reactors the effects of particle stacking are unavoidable, as gas-phase pyrolysis products do not move as quickly through the

sample bed as does sweep gas. Gonenc et al.<sup>16</sup> showed that char yield decreased equivalently when sweep-gas velocity was increased 100-fold as when bed depth was decreased just 5-fold. This is because gas-phase tars move through the sample bed in a manner reminiscent of size-exclusion chromatography, with sweep gas acting as the mobile phase: tar vapours continually adsorb and desorb onto the surface of chars as they move through the complex-and-evolving pore structures of the fixed sample bed.<sup>20</sup>

### *1.2. Thermogravimetric Balance Configuration*

TG balances, commercially available instruments used for TGA, typically consist of a small platinum or ceramic sample pan hanging from a balance hook inside a sealed furnace. Not only are particles in this sample pan stacked, but gas does not flow through the bed (helping to sweep gas-phase products out of the sample matrix) but rather over top, or up and around the sample pan.<sup>21</sup> For this reason, TG balances lead to particularly slow convective mass transfer of gas-phase pyrolysis products out of the sample bed, and therefore emphasise the effects of interphase-mass-transfer-related parameters (particle and sample-bed morphology) on the extent of repolymerisation, and thus on char yield. Char yields from these devices are therefore not representative of the primary pyrolysis behaviour of the sample material, and are sensitive to experimental parameters which influence the residence time of gas-phase products in close proximity to char particles, and thereby the extent of interphase mass transfer (tar condensation onto chars allowing repolymerisation). Here, we vary one such parameter (bed depth via sample mass) in order to quantify this sensitivity, as well as that of other common analyses of biomass thermogravimetry, including kinetic modelling and proximate analysis.

## **2. Experimental**

### *2.1. Materials*

In order to resolve the general influence of interphase-mass-transfer-related parameters on the results of typical TG analyses, the present study has utilised a variety of starting materials. 50  $\mu\text{m}$  particle size microcrystalline cellulose (Sigma-Aldrich, CAS No. 9004-34-6) was used as a replicable standard because it is the primary component of most biomass, and

is readily commercially available. Additionally, birch wood hydrochars produced at different hydrothermal carbonization (HTC) temperatures (160, 180, 200, 220, 230, 240, 260 and 280 °C) and a residence time of 1 hr, were employed to investigate the influence of fixed carbon content on the sensitivity of proximate analysis results to the previously described effects.

## 2.2. Thermogravimetric Analysis of Cellulose

Samples of microcrystalline cellulose between 1 mg and 20 mg were prepared in 100  $\mu$ L platinum sample pans. In a TA Instruments Q500 TGA (Mettler-Toledo Ltd., 64 Boston Road, Beaumont Leys, Leicester, LE4 1AW), samples were held at room temperature in nitrogen for 15 min, then heated at 15 °C min<sup>-1</sup> to 105 °C, and held at this temperature for 20 min. The mass of sample remaining after this program was termed the *dry mass*. Samples were then heated at rates between 2 °C min<sup>-1</sup> and 15 °C min<sup>-1</sup> to peak temperatures between 300 °C and 450 °C, and held at peak temperature for 30 min. The mass of sample remaining after this program was termed the *pyrolysed mass*.

### 2.2.1. Yield Calculations

Cellulose was found to contain no ash via proximate analysis (see section 2.3), so *char yield* was determined on a dry ash-free (daf) basis as *pyrolysed mass/dry mass*. From this, conversion,  $\alpha$ , was calculated as  $1 - \text{char yield}$  and *mass loss* as  $\alpha \times 100\%$ . This is a time-based yield, but as the TGA program has both isothermal and non-isothermal regimes, a temperature-based yield parameter provides additional information.  $T_{50}$  and  $R_{50}$  are the temperature at which *mass loss* = 50%, and the rate of mass loss at that temperature, respectively.<sup>22</sup>

### 2.2.2. Kinetic Calculations

Pre-exponential factor,  $A$ , and activation energy,  $E$ , were calculated using the Kissinger method<sup>23</sup>—the most extensively used multiple-heating-rate model-free method of determining kinetic parameters from thermogravimetry.<sup>24</sup> This method was applied to a first-order reaction model according to International Confederation for Thermal Analysis and Calorimetry (ICTAC) Kinetics Committee recommendations for performing kinetic

computations on thermal analysis data.<sup>24</sup> The governing relation for this model is described by eq. (1), where  $\beta$  is the heating rate,  $T_m$  is the temperature at the maximum degradation rate, and  $R$  is the gas constant.

$$\ln \frac{\beta}{T_m^2} = \ln \frac{AR}{E} - \frac{E}{RT_m} \quad (1)$$

From eq. (1),  $E$  and  $A$  can be determined from the slope and intercept, respectively, of a plot of  $\ln \beta/T_m^2$  vs.  $1/T_m$ . Several assumptions underlie this governing relation:

1. Reaction rate,  $d\alpha/dt$ , is maximised. Temperature at this maximum rate is  $T_m$  and conversion is  $\alpha_m$ .
2. Reaction rate depends on temperature and conversion. Temperature dependence is determined by the Arrhenius equation for non-isothermal processes, and conversion dependence is determined by first-order process kinetics. The validity of the first-order assumption was tested by measuring the dependence  $\alpha_m$  on  $\beta$ . No dependence indicates validity of the assumption.<sup>24</sup>
3. Degradation is a single kinetic step. The validity of this single-step assumption was tested by comparing values of  $E$  extracted from eq. (1) with those from a plot of  $\ln \Delta t_{1/2}$  vs.  $1/T_m$ , where  $\Delta t_{1/2}$  is the width at half height of the differential thermogravimetry (DTG) peak,  $d\alpha/dt$ . Close agreement of these values indicates validity of the assumption.<sup>25</sup>

### 2.3. Proximate Analysis of Birch Wood Hydrochars

Hydrothermal carbonization of birch wood was carried out in a 50 mL stainless steel batch reactor<sup>26</sup> at eight different temperatures ranging from 160 to 280 °C with a fixed residence time of 1 hr, and a biomass to water mass ratio of 30%. Hydrochar samples were recovered via filtration and dried in a ventilated oven at 105 °C overnight before use.

Proximate analysis of birch wood hydrochars was performed in a TA Instruments Q500 TGA using a modified version of the TGA program described by ASTM D7582<sup>27</sup>, which lays out standards for proximate analysis of coal and coke via TGA. This method has also been shown

to produce consistent results when applied to biomass.<sup>1,2</sup> A slower TGA program based on this standard was developed to ensure ample time for heat transfer from the surrounding gas to the sample bed; this program is detailed below.

1. Drying: 2 mg and 20 mg samples were held at room temperature in nitrogen for 15 min, then heated at 15 °C min<sup>-1</sup> to 105 °C, and held at this temperature for 20 min. The mass of sample remaining after this program was termed the *dry mass*.
2. Pyrolysis: Dried samples were heated at 15 °C min<sup>-1</sup> to 900 °C, held at this temperature for 7 min, and then cooled at 15 °C min<sup>-1</sup> to 450 °C. The mass of sample remaining after this program was termed the *pyrolysed mass*.
3. Combustion: Pyrolysed samples were heated at 15 °C min<sup>-1</sup> to 750 °C in air, and held at this temperature for 15 min. The mass of sample remaining after this program was termed the *ash mass*, and the *daf mass* was determined as *dry mass* – *ash mass*.

*Volatile matter* was then determined as  $(\text{dry mass} - \text{pyrolysed mass}) / \text{daf mass} \times 100\%$ , and *fixed carbon* as  $(\text{pyrolysed mass} - \text{ash mass}) / \text{daf mass} \times 100\%$ .

### 3. Results and Discussion

#### 3.1. Yield Analysis

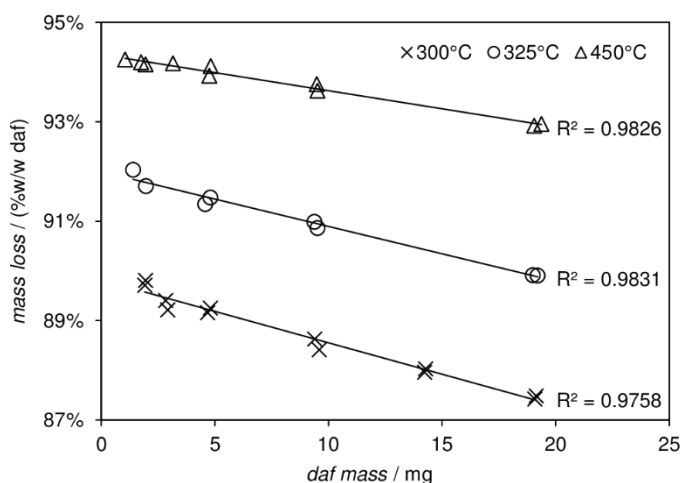


Figure 1: *mass loss* of cellulose on pyrolysis via TG balance by sample mass. Samples of 50  $\mu\text{m}$  particle size microcrystalline cellulose between 1 mg and 20 mg were heated at rate of 2  $^{\circ}\text{C min}^{-1}$  in nitrogen to peak temperatures between 300  $^{\circ}\text{C}$  and 450  $^{\circ}\text{C}$ , and held at peak temperature for 30 min. daf: dry ash-free.

Figure 1 shows that *mass loss* of cellulose, during pyrolysis via TG balance to peak temperatures between 300  $^{\circ}\text{C}$  and 450  $^{\circ}\text{C}$ , followed by a 30 min hold at peak temperature, was found to decrease linearly with sample mass ( $1 \text{ mg} \leq \text{daf mass} \leq 20 \text{ mg}$ ). While the 1 to 3 p.p. (percentage point) maximum effect is relatively small, it is clear from fig. 1 that this magnitude is greater than that of experimental error. This trend is the result of increased repolymerisation upon increased interphase mass transfer caused by increasing bed depth via sample mass. While such a trend could also indicate increasing thermal lag of the sample bed with increasing depth, this is unlikely to be the case at a heating rate of 2  $^{\circ}\text{C min}^{-1}$ . Richter and Rein<sup>28</sup> have performed a thorough analysis of the microscale effects of heat transfer limitations on cellulose pyrolysis in TG balances, and have determined the critical mass, above which the temperature difference between the sample bed and surrounding gas (thermal lag) is greater than 1  $^{\circ}\text{C}$ , for heating rates up to 100  $^{\circ}\text{C min}^{-1}$ . Assuming perfect thermal contact with surroundings to ensure a conservative estimate, the critical mass for a heating rate of 2  $^{\circ}\text{C min}^{-1}$  was predicted to be greater than 50 mg.

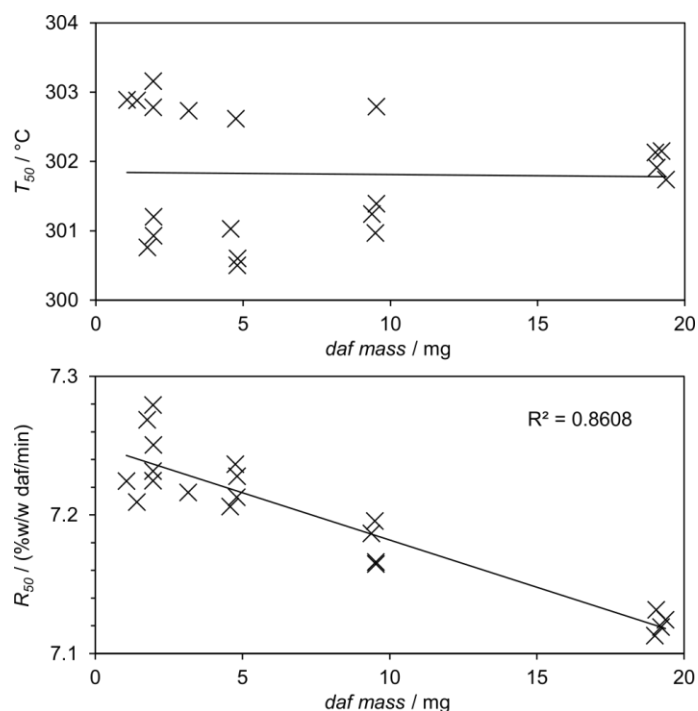


Figure 2:  $T_{50}$  and  $R_{50}$  of cellulose via TGA by sample mass. Samples of 50  $\mu\text{m}$  particle size microcrystalline cellulose between 1 mg and 20 mg were heated at rate of 2  $^{\circ}\text{C min}^{-1}$  in nitrogen.  $T_{50}$ : the temperature at which 50% of *daf mass* has been lost, assuming *daf mass* = *dry mass*.  $R_{50}$ : the rate of mass loss at  $T_{50}$ . daf: dry ash-free.

Another indication the system was not heat-transfer limited during these tests are the trends of  $T_{50}$  and  $R_{50}$  with respect to sample mass. Figure 2 shows that  $R_{50}$  was found to decrease with sample mass, while  $T_{50}$  did not show a clear trend. This indicates that the temperature at which cellulose degradation occurs is not affected by bed depth, but that the rate of this degradation is. Were the decreasing mass loss trend a function of increasing heat transfer limitation,  $T_{50}$  would surely be affected as the recorded temperature became increasingly far from that of the sample bed. The decreasing  $R_{50}$  trend is consistent with increased rates of repolymerisation (which acts as the reverse degradation reaction) upon increasing bed depth.

While it is clear from fig. 1 and fig. 2 that the magnitude of the effects of bed depth on these yield-based parameters is small, this variation is amplified when yield data are differentiated to calculate kinetic parameters. Section 3.2 demonstrates the effects of bed depth on kinetic predictions based on these parameters.



### 3.2. Kinetic Analysis

Pre-exponential factors were determined from intercepts of the Kissinger plots pictured in fig. 3(a) for 2 mg and 20 mg samples of cellulose as  $2.96 \times 10^{16} \text{ min}^{-1}$  and  $2.57 \times 10^{13} \text{ min}^{-1}$ , respectively. Activation energies for 2 mg and 20 mg samples were calculated from slopes of the Kissinger plots as  $190 \text{ kJ mol}^{-1}$  and  $158 \text{ kJ mol}^{-1}$ , respectively. Figure 3(a) shows that while overall agreement between slopes of the Kissinger and  $\ln \Delta t_{1/2}$  plots are reasonable, some deviation is visible, particularly in the bottom-right-hand corner of both the 2 mg and 20 mg axes. This indicates some error in the assumption that pyrolysis of cellulose proceeds as a single step.<sup>25</sup> This is expected, given that cellulose is thought to pyrolyse via a complex network of competing pathways. In particular, at low temperatures, dehydration reactions are thought to dominate, but as temperature increases, depolymerisation reactions (which allow for repolymerisation to occur) take over.<sup>29, 30</sup> As heating rate changes, so does the time spent in these regimes, causing changes to the shapes of DTG peaks, which are picked up by the peak-width-based  $\ln \Delta t_{1/2}$  analysis. Quantitatively, this error corresponds to a 9 to 11% deviation in  $E$ . Compared to the observed 17% variation in  $E$  due to sample mass, this relatively substantial error suggests that the single-step approximation is not valid. However, the Kissinger method is often used without verifying this assumption,<sup>5-7</sup> which is even less applicable when multiple lignocellulosic components are present, so predictions using the above parameters are still indicative of the magnitude of variation due to bed depth of typical kinetic analyses of TG data resulting from the repolymerisation-emphasising configuration of TG balances.

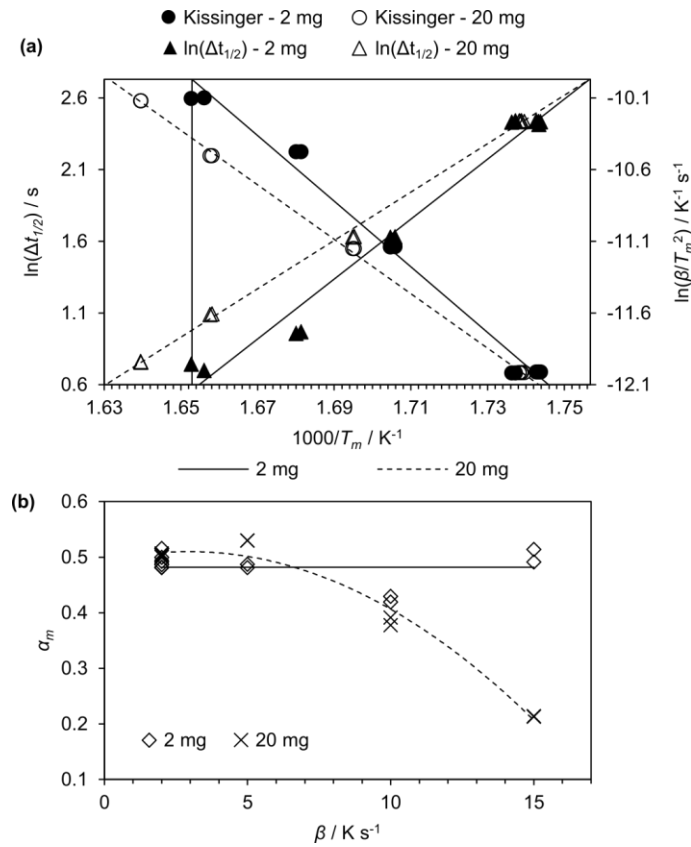


Figure 3: Tests of the single-step (a) and first-order (b) assumptions applied to extract kinetic parameters from thermogravimetry data using the Kissinger method. (a) Combined Kissinger ( $\bullet, \circ$ ) and  $\ln \Delta t_{1/2}$  (plots for pyrolysis of cellulose via TG balance at heating rates between 2  $^{\circ}C \text{ min}^{-1}$  and 15  $^{\circ}C \text{ min}^{-1}$ . Black symbols ( $\bullet, \blacktriangle$ ) refer to 2 mg sample results, and 2 mg kinetic parameters (pre-exponential factor and activation energy) are determined by the solid lines on the restricted axis. White symbols ( $\circ, \triangle$ ) refer to 20 mg sample results, and 20 mg kinetic parameters are determined by the dashed lines. Divergence of line intercepts from corners of the defined axes indicate error in the single step assumption.  $\Delta t_{1/2}$ : differential thermogravimetry peak width at half height;  $T_m$ : temperature at maximum reaction rate. (b) Results of the first-order assumption test for 2 mg ( $\diamond$ ) and 20 mg ( $\times$ ) samples. Solid and dashed lines are approximate models of the dependence of conversion at maximum reaction rate ( $\alpha_m$ ) on heating rate ( $\beta$ ) of 2 mg and 20 mg samples, respectively. Dependence indicates error in the first-order assumption.

Figure 3(b) shows that while  $\alpha_m$  is not dependent on heating rate for 2 mg samples, it decreases with heating rates greater than 5  $^{\circ}C \text{ min}^{-1}$  for 20 mg samples. At 15  $^{\circ}C \text{ min}^{-1}$ , 20 mg samples lost approximately 58% less mass by the time their rate of mass loss was maximised

than 2 mg samples did. This dependence indicates error in the assumption that the pyrolysis of cellulose is approximately first-order,<sup>24</sup> but only for 20 mg samples at higher heating rates. Repolymerisation, taken as an elementary step, relies on multiple reactants to produce a single polymer, and is thus unlikely to follow first-order kinetics. This may indicate that within this range of very slow heating rates, there is a threshold below which the effect of bed depth on repolymerisation is minimal. This could be due to decreased volatilisation of tars at lower heating rates, so that repolymerisation is less dependent on interphase mass transfer (condensation) and related experimental parameters. However, heating-rate dependence of the effect of sample mass on  $T_m$  was also observed (see fig. 3(a) Kissinger plots), which could indicate that these dependencies are related to heat transfer limitations. Richter and Rein<sup>28</sup> characterise a 20 mg sample heated at 15 °C min<sup>-1</sup> as experiencing approximately 1 °C thermal lag, while the observed variation in  $T_m$  was approximately 5 to 6 °C, so it is likely that this heating-rate dependence is at least partially related to mechanistic effects. Despite the first-order approximation failing for 20 mg, 15 °C min<sup>-1</sup> samples, removing these from the Kissinger plot does not substantially affect results of this analysis, so kinetic predictions have been made with the previously stated parameters.

Figure 4(a) depicts the difference between models of rate constant as a function of temperature,  $k(T) = A \exp(-E/RT)$ , produced from 2 mg and 20 mg kinetic parameters. The models predict that a 20 mg sample will degrade up to two orders of magnitude more quickly at low temperatures (100 °C to 281 °C), and more slowly at high temperatures (281 °C to 1000 °C), than a 2 mg sample. Figure 4(b) shows that while this trend was confirmed experimentally ( $\alpha$  equivalence point within 15 °C of the model in this case), the magnitude of the effect at low temperatures was overpredicted by the models. Furthermore, the models overpredicted *mass loss* by 7 to 9 p.p. and underpredicted the maximum difference in conversion between the two models,  $(\Delta\alpha)_{max}$ , by approximately 40%. Though the models underpredicted the magnitude of the effect of sample mass in the case of very slow heating to relatively low temperatures, fig. 4(c) and fig. 4(d), respectively, show that the models substantially diverge in the case of flash heating (1000 °C s<sup>-1</sup>) and high temperature holds (1000 °C). Flash heating produced a

$(\Delta\alpha)_{max}$  of approximately 0.52 in around 0.4 s, and holding at 1000 °C produced a  $(\Delta\alpha)_{max}$  of approximately 0.91 in around 0.5  $\mu$ s.

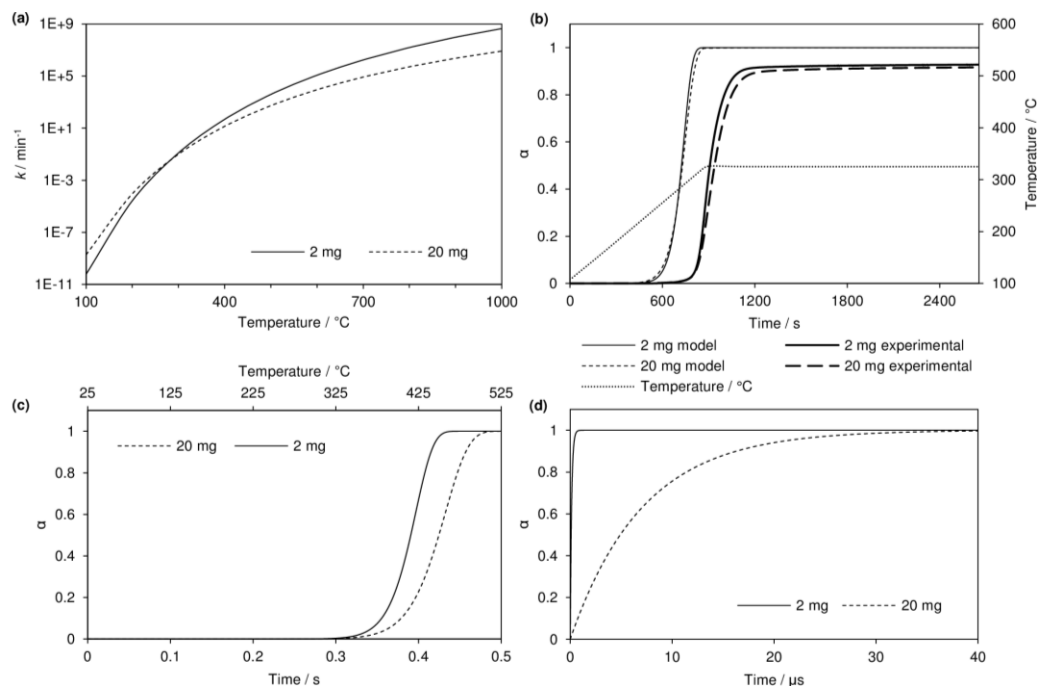


Figure 4: Kinetic predictions of cellulose pyrolysis based on kinetic parameters calculated from 2 mg and 20 mg samples. (a) Rate constant,  $k$ , as a function of temperature by sample mass. (b) Fit of kinetic models to thermogravimetry data by sample mass. Cellulose was heated from 105 °C to 325 °C at a rate of 15 °C min<sup>-1</sup>, and then held at 325 °C for 30 min.  $\alpha$ : conversion on a dry ash-free basis. (c) Kinetic predictions for heating cellulose from 25 °C to 525 °C at a rate of 1000 °C s<sup>-1</sup> by sample mass. (d) Kinetic predictions for holding cellulose at 1000 °C for 40  $\mu$ s by sample mass.

### 3.3. Proximate Analysis

Figure 5 shows that a ten-fold increase in bed depth led to a 3 to 6 p.p. increase in *fixed carbon* and decrease in *volatile matter* of birch wood chars over the entire range of hydrothermal carbonisation (HTC) temperatures tested (160 °C to 280 °C). This effect was found to generally increase with HTC temperature, which is likely attributable to the greater proportion of *fixed carbon* in higher-temperature samples, allowing more char contact per unit volatilised tar, but could also be due to differences in char nature and/or morphology reducing

tar-cracking phenomena. However, higher HTC temperatures lead to lower hydrochar surface area and porosity due to the greater amount of spheroidal secondary char produced.<sup>31-33</sup> Thus, it is unlikely that morphology is the cause of the greater extent of repolymerisation in higher HTC temperature hydrochars. These results are consistent with increased repolymerisation as a function of increased bed depth, and represent substantial unreliability in this method of proximate analysis. The magnitude of this variation in proximate composition due to sample mass was between 8% and 16% of that due to the entire HTC process at 280 °C. Circumventing this error is not as simple as using a small and consistent sample size for proximate analysis, because the vast majority of 2 mg samples were insufficient to resolve ash content, which was revealed to be present with a discernible trend with respect to HTC temperature by the 20 mg sample results. It is also not feasible to simply apply a “fudge factor” to higher-sample-mass results, because the effect of sample mass is not constant with respect to sample composition, as demonstrated by the trend of this effect with respect to HTC temperature.

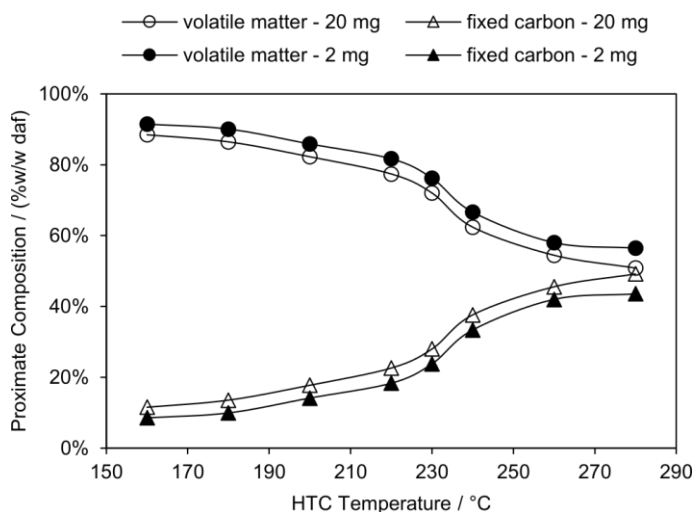


Figure 5: Proximate composition of birch wood chars by hydrothermal carbonisation (HTC) temperature and sample mass. ●,○: *volatile matter* content of 2 mg and 20 mg samples, respectively. ▲,△: *fixed carbon* content of 2 mg and 20 mg samples, respectively. daf: dry ash-free.

#### **4. Conclusions**

1. Product distributions from pyrolysis of cellulose via TG balance are sensitive to variations in sample mass due to this device's configuration emphasising the effect of bed depth on extent of tar repolymerisation.
2. Despite simple kinetic models derived from TGA underpredicting this sensitivity under typical TGA conditions, high heating rate and high temperature conditions greatly amplify this sensitivity.
3. Proximate analysis of biomass via TG balance is also sensitive to variations in sample mass.
4. This sensitivity means the results of these typical TG analyses are not fundamental properties of the material tested when a single sample mass is used.
5. This sensitivity is present in all fixed-bed reactors as a result of particle stacking. Guidelines for minimizing this sensitivity in fixed-bed reactors are needed, and future work will focus on identifying these.

#### **5. Conflicts of Interest**

There are no conflicts to declare.

#### **6. Acknowledgements**

The authors would like to thank Prof Rafael Kandiyoti for helping to inspire this work and Paul-Enguerrand Fady for proofreading. Funding: This work was supported by Queen Mary University of London.

#### **7. References**

1. J. Cai, Y. He, X. Yu, S. W. Banks, Y. Yang, X. Zhang, Y. Yu, R. Liu, A. V. Bridgwater, Review of physicochemical properties and analytical characterization of lignocellulosic biomass, *Renewable and Sustainable Energy Reviews* 76 (2017) 309–322. doi:10.1016/j.rser.2017.03.072.
2. R. Garcia, C. Pizarro, A. G. Lavin, J. L. Bueno, Biomass proximate analysis using thermogravimetry, *Bioresource Technology* 139 (2013) 1–4. doi:10.1016/j.biortech.2013.03.197.

3. R. Volpe, A. Messineo, M. Millan, Carbon reactivity in biomass thermal breakdown, *Fuel* 183 (2016) 139–144. doi:10.1016/j.fuel.2016.06.044.
4. R. Volpe, J. M. B. Menendez, T. R. Reina, A. Messineo, M. Millan, Evolution of chars during slow pyrolysis of citrus waste, *Fuel Processing Technology* 158 (2017) 255–263. doi:10.1016/j.fuproc.2017.01.015.
5. L. Abdelouahed, S. Leveneur, L. Vernieres-Hassimi, L. Balland, B. Taouk, Comparative investigation for the determination of kinetic parameters for biomass pyrolysis by thermogravimetric analysis, *Journal of Thermal Analysis and Calorimetry* 129 (2017) 1201–1213. doi:10.1007/s10973-017-6212-9.
6. A. Mabuda, N. Mamphweli, E. Meyer, Model free kinetic analysis of biomass/sorbent blends for gasification purposes, *Renewable and Sustainable Energy Reviews* 53 (2016) 1656–1664. doi:10.1016/j.rser. 2015.07.038.
7. K. Slopiecka, P. Bartocci, F. Fantozzi, Thermogravimetric analysis and kinetic study of poplar wood pyrolysis, *Applied Energy* 97 (2012) 491– 497. doi:10.1016/j.apenergy.2011.12.056.
8. D. Ferdous, A. K. Dalai, S. K. Bej, R. W. Thring, Pyrolysis of Lignins: Experimental and Kinetics Studies, *Energy & Fuels* 16 (2002) 1405– 1412. doi:10.1021/ef0200323.
9. T. Sonobe, N. Worasuwanarak, Kinetic analyses of biomass pyrolysis using the distributed activation energy model, *Fuel* 87 (2008) 414–421. doi:10.1016/j.fuel.2007.05.004.
10. R. Kandiyoti, Reply to Letter to the Editor by Sun et al. [FUEL/2001/0120 (Letter)]: The synergistic effect between macerals during pyrolysis, *Fuel* 81 (2002) 975. doi:10.1016/S0016-2361(01) 00206-X.
11. P. Brandt, E. Larsen, U. Henriksen, High tar reduction in a two-stage gasifier, *Energy & Fuels* 14 (2000) 816–819. doi:10.1021/ef990182m.
12. F. Dabai, N. Paterson, M. Millan, P. Fennell, R. Kandiyoti, Tar Formation and Destruction in a Fixed-Bed Reactor Simulating Downdraft Gasification: Equipment Development and Characterization of TarCracking Products, *Energy & Fuels* 24 (2010) 4560–4570. doi:10.1021/ ef100681u.
13. F. Dabai, N. Paterson, M. Millan, P. Fennell, R. Kandiyoti, Tar Formation and Destruction in a Fixed Bed Reactor Simulating Downdraft Gasification: Effect of Reaction Conditions on Tar Cracking Products, *Energy & Fuels* 28 (2014) 1970–1982. doi:10.1021/ef402293m.
14. S. M. Nunes, N. Paterson, D. R. Dugwell, R. Kandiyoti, Tar Formation and Destruction in a Simulated Downdraft, Fixed-Bed Gasifier: Reactor Design and Initial Results, *Energy & Fuels* 21 (2007) 3028–3035. doi:10. 1021/ef070137b.

15. S. M. Nunes, N. Paterson, A. A. Herod, D. R. Dugwell, R. Kandiyoti, Tar Formation and Destruction in a Fixed Bed Reactor Simulating Downdraft Gasification: Optimization of Conditions, *Energy & Fuels* 22 (2008) 1955–1964. doi:10.1021/ef700662g.
16. Z. Gonenc, J. R. Gibbins, I. E. Katheklakis, R. Kandiyoti, Comparison of coal pyrolysis product distributions from three captive sample techniques, *Fuel* 69 (1990) 383–390. doi:10.1016/0016-2361(90)90104-X.
17. W. S. L. Mok, M. J. Antal, P. Szabo, G. Varhegyi, B. Zelei, Formation of charcoal from biomass in a sealed reactor, *Industrial & Engineering Chemistry Research* 31 (1992) 1162–1166. doi:10.1021/ie00004a027.
18. J. Recari, C. Berruero, S. Abello, D. Montane, X. Farriol, Effect of temperature and pressure on characteristics and reactivity of biomass-derived chars, *Bioresource Technology* 170 (2014) 204–210. doi:10.1016/j.biortech.2014.07.080.
19. N. Zobel, A. Anca-Couce, Slow pyrolysis of wood particles: Characterization of volatiles by Laser-Induced Fluorescence, *Proceedings of the Combustion Institute* 34 (2013) 2355–2362. doi:10.1016/j.proci.2012.06.130.
20. D. Griffiths, J. Mainhood, The tar cracking of tar vapor and aromatic compounds on activated carbon, *Fuel* 46 (1967) 167–176.
21. Thermal Advantage, TA Instruments: Thermal Analysis, 2006. URL: <http://www.tainstruments.com/pdf/TGABrochure.pdf>.
22. W.-H. Chen, P.-C. Kuo, A study on torrefaction of various biomass materials and its impact on lignocellulosic structure simulated by a thermogravimetry, *Energy* 35 (2010) 2580–2586. doi:10.1016/j.energy.2010.02.054.
23. H. E. Kissinger, Reaction Kinetics in Differential Thermal Analysis, *Analytical Chemistry* 29 (1957) 1702–1706. doi:10.1021/ac60131a045.
24. S. Vyazovkin, A. K. Burnham, J. M. Criado, L. A. P´erez-Maqueda, C. Popescu, N. Sbirrazzuoli, ICTAC Kinetics Committee recommendations for performing kinetic computations on thermal analysis data, *Thermochimica Acta* 520 (2011) 1–19. doi:10.1016/j.tca.2011.03.034.
25. J. Farjas, N. Butchosa, P. Roura, A simple kinetic method for the determination of the reaction model from non-isothermal experiments, *Journal of Thermal Analysis and Calorimetry* 102 (2010) 615–625. doi:10.1007/s10973-010-0737-5.
26. L. Fiori, D. Basso, D. Castello, M. Baratieri, Hydrothermal carbonization of biomass: Design of a batch reactor and preliminary experimental results, *Chem. Eng. Trans.* 37 (2014) 55–60. doi:10.3303/CET1437010.



27. ASTM International, ASTM D7582 - 15: Standard Test Methods for Proximate Analysis of Coal and Coke by Macro Thermogravimetric Analysis, Technical Report, West Conshohocken, PA, 2015. doi:10.1520/D7582-15.
28. F. Richter, G. Rein, The Role of Heat Transfer Limitations in Polymer Pyrolysis at the Microscale, *Frontiers in Mechanical Engineering* 4 (2018) 18. doi:10.3389/fmech.2018.00018.
29. F. J. Kilzer, A. Broido, Speculations on the Nature of Cellulose Pyrolysis, *Pyrodynamics* 2 (1965) 151–163.
30. Volpe R., Messineo S., Volpe M., Messineo A., Catalytic effect of char for tar cracking in pyrolysis of citrus wastes, design of a novel experimental set up and first results. *Chemical Engineering Transactions* 50 (2016) 181-186
31. M. Lucian, M. Volpe, L. Gao, G. Piro, J.L. Goldfarb, L. Fiori, Impact of hydrothermal carbonization conditions on the formation of hydrochars and secondary chars from the organic fraction of municipal solid waste, *Fuel*. 233 (2018) 257–268. doi:10.1016/j.fuel.2018.06.060.
32. Volpe, M., Fiori, L., Volpe, R., Messineo, A., 2016. Upgrading of Olive Tree Trimmings Residue as Biofuel by Hydrothermal Carbonization and Torrefaction : a Comparative Study 50, 13–18. doi:10.3303/CET1650003
33. M. Volpe, L. Fiori, From olive waste to solid biofuel through hydrothermal carbonisation: The role of temperature and solid load on secondary char formation and hydrochar energy properties, *J. Anal. Appl. Pyrolysis*. 124 (2017) 63–72. doi:10.1016/j.jaap.2017.02.022.